Journal of Engineering
journal homepage: www.joe.uobaghdad.edu.iq
Number 5 Volume 26 May 2020

Civil and Architectural Engineering

Effect of Maximum Size of Aggregate on the Behavior of Reinforced Concrete Beams Analyzed using Meso Scale Modeling

Eman Abbas*
Ph.D. student
College of Engineering-University of Baghdad
Email: dremancivil2019@gmail.com

Alaa H. AlZuhairi
Asst. Prof. Dr.
College of Engineering-University of Baghdad
Email:alaalwn@coeng.uobaghdad.edu.iq

ABSTRACT

In this study, simply supported reinforced concrete (RC) beams were analyzed using the Extended Finite Element Method (XFEM). This is a powerful method that is used for the treatment of discontinuities resulting from the fracture process and crack propagation in concrete. The mesoscale is used in modeling concrete as a two-phasic material of coarse aggregate and cement mortar. Air voids in the cement paste will also be modeled. The coarse aggregate used in the casting of these beams is a rounded aggregate consisting of different maximum sizes. The maximum size is 25 mm in the first model, and in the second model, the maximum size is 20 mm. The compressive strength used in these beams is equal to 26 MPa.
The subjects of this study are two RC beams subjected to a two-point loading designed to fail due to flexure. The RC beams under loading were studied in the laboratory as well as numerically. ABAQUS program was used for modeling and analyzing the RC beams. The mesoscale modeling that was used to model the concrete required used a special program using different programs but has not used the ABAQUS program directly. The result of the comparison between the numerical and experimental showed that the mesoscale numerical model gave results that were more approximate to the experimental ones, and the mesoscale modeling of reinforced concrete is most convenient when the maximum size of aggregate is decreased.
Keywords: Extended Finite Element Method, Fracture mechanics, Meso scale modeling, Crack propagation.

تأثير المقاس الاقصى للركام على سلوك الاعتاب الخرسانيه المسلحة التي تم تحليلها بأستخدام انموذج النطاق متوسط المدى

د. علاء حسين الزهيري
استاذ مساعد
كلية العندسة – جامعة بغداد

ايمان عباس
طالبة دكتوراه
كلية الهندسة – جامعة بغداد

الخلاصة

في هذه الدراسة, تم تحليل الاعتاب الخرسانة المسلحة (RC) المسندة أسنادا بسيطا (Simply Supported) بأستخدام طريقة العناصر المحددة الممتدة (XFEM).الطريقة هذه تكون فعالة حيث تستخدم للتعامل مع حالات عدم الاستمرارية الناتجة من

*Corresponding author
Peer review under the responsibility of University of Baghdad.
https://doi.org/10.31026/j.eng.2020.05.10

Article received: 14 /7/2019
Article accepted: 1/10 /2019
Article published:1/5/2020

عملية الكسر وانتشار الشقوق في الخرسانة. يستخدم النطاق متوسط المدى لنمذجة الخرسانة كمادة ثنائية الطور تتكون من الركام الخشن والعجينة الاسمنتية. كذلك سيتم نمذجة الفراغات الهوائية الموجودة في عجينة الاسمنت.
الركام الخشن المستخدم لصب الاعتاب هو ركام مدور لكن مختلف بالمقاس الاقصى. في النموذج الاول استخدم ركام بمقاس اقصى 25 ملم وفي النموذج الثاني استخدم ركام ذو مقاس اقصى 20 ملم. مقدار مقاومة الانضغاط لهذه الاعتاب هي 26 ميكاباسكال.
سيتم دراسة اثنين من الاعتاب الخرسانية المسلحة المعرضة للتحميل النقطي الثنائي تم تصميمها لتفشل نتيجة الانحناء. الاعتاب الخرسانية المسلحة تم دراستها مختبريا وكذلك بشكل عددي. استخدم برنامج (ABAQUS) لنمذجة وتحليل الاعتاب الخرسانية المسلحة. لنمذجة الخرسانة بأستخدام النطاق المتوسط المدى (Meso-Scale) تطلب أستخدام برمجة خاصة بأستخدام برامج اخرى ولم يتم استخدام برنامج ال ABAQUS يشكل مباشر للبرمجه. اظهرت مقارنة النتائج العددية مع المختبرية بان النمذجة بأستخدام النطاق المتوسط المدى يعطي نتائج متقاربة جدا من النتائج المحسوبة مختبريا.
الكلمات الرئيسية:طريقة العناصر المحددة الممتدة, ميكانيك الكسر, النمذجة المتوسطة المدى, انتشار الشقوق.

1. INTRODUCTION

Concrete is a non-homogenous material (heterogeneous material), wherein it consists of coarse aggregate, cement mortar, and air voids in the cement paste. This property makes the behavior of concrete depend upon the behavior of the material (components).

In many studies, concrete is assumed to be a homogenous material for simplicity and is modeled on a macro scale, but to understand the behavior of concrete, many analytical scales were developed, such as meso, micro, and atomic scales. The mesoscale analysis model gives a good indicator of the behavior of the concrete. In the mesoscale structures, concrete is considered as a multiphase material **(Al-Zuhairi and Taj (a), 2018)**, **(Al-Zuhairi and Taj (b), 2018)**.

In this paper, two reinforced concrete beams with dimensions of 350 × 200 × 2200 mm will be analyzed numerically by using the Extended Finite Element Method (XFEM). The results of the two models will be compared with the experimental results of the same reinforced concrete beams with approximately the same compositions. Effect of the maximum size of aggregate on the behavior of RC beams under bending analysis using mesoscale will be studied.

2. THE MESO SCALE MODELING

The mesoscale is a scale that falls between the macro and micro scales **(Murayama, 2001),** as in **Fig.1**. The continuum and the lattice models are subdivisions of the mesoscale modeling. In the continuum models, the material is divided into components; for example, concrete consisting of aggregate, mortar, and the interface zone between the two materials **(Liao et al., 2004)**. In this paper, this model will be used for modeling concrete as aggregate, mortar, and air voids that result from the pouring process of concrete. The interface between the aggregate and cement mortar is modeled as fully bound and tied. This assumption is not really correct because the micro-cracks start from these areas (transition zone or the interface between the aggregate and cement paste) and form weak points in concrete. Still, this study is a start to study mesoscale in the RC beams. The lattice models of concrete are modeled as a discrete system consisting of a lattice element **(Nitka and Tejchman, 2015)**. This model needs a massive numerical effort to model concrete.

The mesoscale modeling has two approaches; image-based and parameterization modeling. The first one approaches the building on a set of 2D pictures that are assembled to get a 3D model, where the numerical model will be conducted based on this 3D model. These approaches have some advantages and disadvantages. The advantages are an accurate method to model the concrete. The disadvantages are an expensive and time-consuming method **(Bentz et al., 1994)**, **(Mostafavi et al., 2013)**, and **(Jivkov et al., 2013)**. The second approach (parameterization) is divided into two methods, direct and indirect. In the direct method, the major parameters are those such as shape, size, gradation, and distribution of the aggregate particles, the interface between aggregate particles and cement mortar, and their effect on the mechanical behavior of the concrete of the multi-phase material computation **(Wang, 2015)**. In the indirect method, the heterogeneity of the concrete is modeled separately with a regular FE mesh **(Yang, 2009)**, or by using lattice modeling for the aggregate and mortar phases **(Leiti, 2003)** and **(Schlangen, 1997)**.

The direct method is more appropriate for the mesoscale modeling process and will be used in this study.

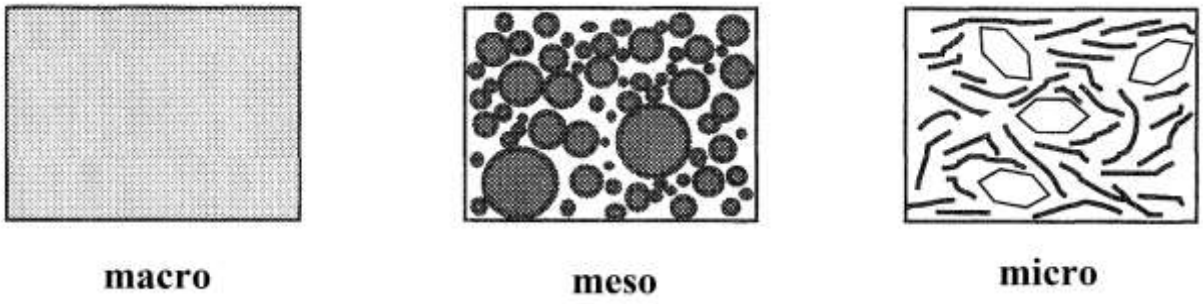

Figure 1. Concrete material structure: macro, meso and micro level.

2. THE EXENDED FINITE ELEMENT ETHOD (XFEM)

The extended finite element method (XFEM) is a numerical method based on the finite element method and on the partition of unity methods (PoUM or PUM). It is the use of partition of unity functions which are functions whose values sum up to unity at each point in the domain **(Ahmed, 2009)**. The XFEM is used to solve the discontinuity problems that occur in brittle materials such as concrete **(Belytschko and Black, 1999)**.

Localized enrichment functions are used in the XFEM, which are an enrichment of nodes and developed near the discontinuity **(Khoei, 2015)**. There are two types of discontinuities in concrete structures. The weak discontinuity and strong discontinuity. Weak discontinuity in concrete results from bi-material problems (aggregate particles and cement mortar). The strong discontinuity is described by the crack interface in the domain **(Khoei, 2015)**.
The enrichment is done mathematically by adding the enrichment part to the standard part of regular interpolation, as shown in Eq. (1)

$$u(x) = \sum_{i=1}^{N} N_i(x) \times \bar{u}_i + enrichment\ terms \quad (1)$$

$$u(x) = \underbrace{\sum_{i=1}^{N} N_i(x) \times \bar{u}_i}_{\text{regular interpolation}} + \underbrace{\sum_{k=1}^{p} \bar{N}_i(x) \times \left(\sum_{j=1}^{M} \psi_j(x) \times \bar{a}_{ij}\right)}_{\text{enrichment interpolation}} \quad (2)$$

Where:
$N_i(x)$: The standard or regular shape functions
$\bar{N}_i(x)$: The enhanced shape functions
$\bar{u}_i$: standard DOF
$\bar{a}_i$: enrichment DOF
N : the set of all nodal points
M : the number of enrichment node
$\psi_j(x)$: the enrichment function
p : the number of enrichment function

3. ENRICHMENT FUNCTION

The enrichment is an act of improving the approximation displacement field based on the properties of the problem. The choosing of the enrichment functions is related to the type of

discontinuity, and its influences on the kinds of solutions. These functions are such as the signed distance function, level set function, branch function, Heaviside jump function, and so on.

The level set function is used for weak discontinuity, where it is the signed distance function $\varphi(x)$.

$$u_{\text{weak discontinuity}}(x) = \sum_{i=1}^{N} N_i(x) \times \bar{u}_i + \sum_{j=1}^{M} N_j(x) \times \left(|\varphi(x)| - \left|\varphi(x_j)\right|\right) \times \bar{a}_j \quad (3)$$

Where

$\varphi(\vec{x})$: is the signed distance to the closest point on the interface

$$\varphi(\vec{x}) = \vec{N} d(\vec{x}) \quad (4)$$

$\vec{N}$: is the local unit normal at $\vec{x}$ taking the value (+,−) that referred to the outside and inside regions.

For modeling the strong discontinuity (cracks), two enrichment functions are used: Heaviside or step function (jump function), and asymptotic near-tip enrichment function (**Belytschko and Black, 1999), and (Khoei (2015**).

$$u_{crack}(x) = \sum_{i \in N} N_i(x) \times \bar{u}_i + \sum_{j \in N^{dis}} N_i(x) \sum_{j=1}^{M} N_j(x) \times \left(H(x) - H(x_j)\right) \times \bar{d}_j +$$

$$\sum_{k \in N^{tip}} N_k(x) \times \sum_{a=1}^{4} (B_a(x) - B_a(x_k)) \times \bar{b}_{ak} \quad (5)$$

Where:

N^{dis} : The set of enriched nodes whose support is bisected by the crack

N^{tip} : The set of nodes which contains the crack tip in the support of their shape functions enriched by the asymptotic functions

$\bar{u}_i$: The unknown standard nodal DOF at I^{th} node

$\bar{d}_j$: The unknown enriched nodal DOF associated with the Heaviside enrichment function at node J

$\bar{b}_{ak}$: The additional enriched nodal DOF associated with the asymptotic functions at node K.

4. EXPERIMENTAL WORK

The experimental work consisted of casting and then testing two simply supported reinforced concrete beams with dimensions of 2200 × 350 × 200 mm using minimum reinforcement, as in **Fig.2**. The first beam used rounded coarse aggregate with a maximum size of 20 mm. The second beam used rounded coarse aggregate with a maximum size of 25 mm. The amounts of the material used to casting these beams are explained in **Table (1)** and were designed and executed according to (ACI 211-02).

These beams are tested under two-point loads, and these beams are designed to fail in flexure.

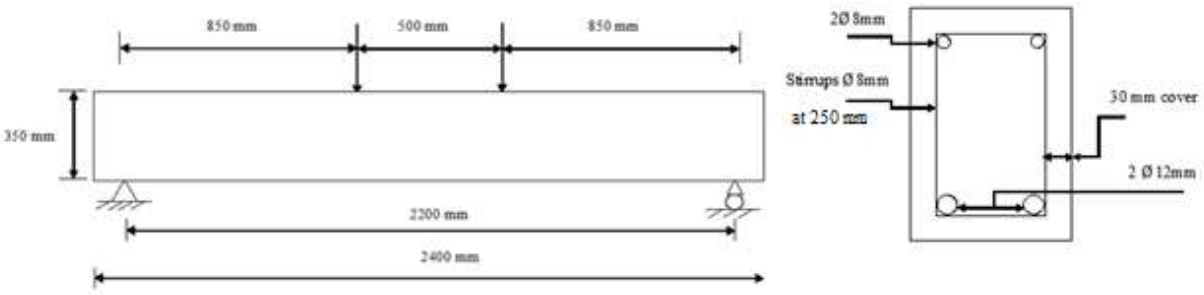

Figure 2. The beam model.

Table 1. Design mix proportions for the concrete beam specimens in the first and second beams.

	First beam	Second beam
Cement kg/m^3	324	344
Coarse Aggregate kg/m^3	1249	1180
Fine Aggregate kg/m^3	553	562
Mixing Water kg/m^3	193	205
Air voids Content %	1.5	2
Density of Coarse Aggregate	1720	1746
Water / Cement	0.6	0.6
Mix ratio	1: 1.7 : 3.85	1 : 1.6 : 3.4

The load was applied incrementally. The amounts of strains and deflection at the beam mid-span corresponding to each load increment were recorded. Two electric strain gauges were attached to each RC beam specimen. One of these gauges was attached in the middle of the front face of the specimens in the tension zone, the other gauge was attached at the middle of the bottom face of the specimens. These two strain gages were used to measure the tensile strain at midspan of RC beam specimens. Dial gauge was used for deflection measurements. It was located at midspan of the bottom face of the RC beam specimens

The first beam, which was constructed using rounded coarse aggregate with a maximum size equal to 25mm, was failed at a load of 106 kN. The first cracking was observed at the midspan at a load of 27 24 kN. This crack is very fine then when the applied load is increased, and other cracks had appeared, **Fig. 3**.

The second beam, which was constructed using rounded coarse aggregate with a maximum size equal to 20mm, was failed at a load of 99.8 kN. The first crack was observed at the mid-span at a load of 24 kN, **Fig. 4**.

Figure 3. The first RC beam testing.

Figure 4. The second RC beam testing.

5. NUMERICAL WORK

Two-dimensional mesoscale finite element models were used in modeling the two RC beams. Concrete was modeled as a bi-phasic material consisting of coarse aggregate particles and cement mortar. Air voids were assumed as spaces (voids) in the concrete model without any material properties **(Al-Zuhairi and Taj (a), and (b), 2018)**.

Fig. 5 explains rounded coarse aggregate with a maximum size of 25 mm, while **Fig. 6** shows the rounded coarse aggregate with a maximum size of 20 mm.

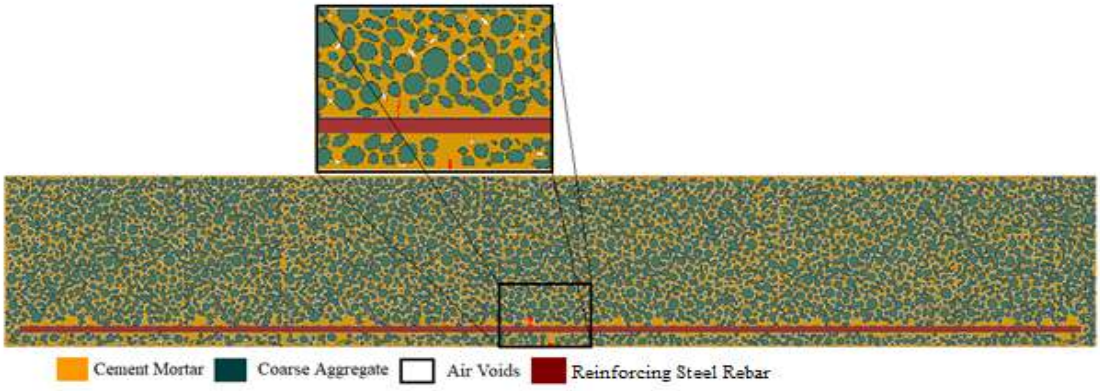

Figure 5. Mesoscale finite element modeling for rounded coarse aggregate with maximum size 25

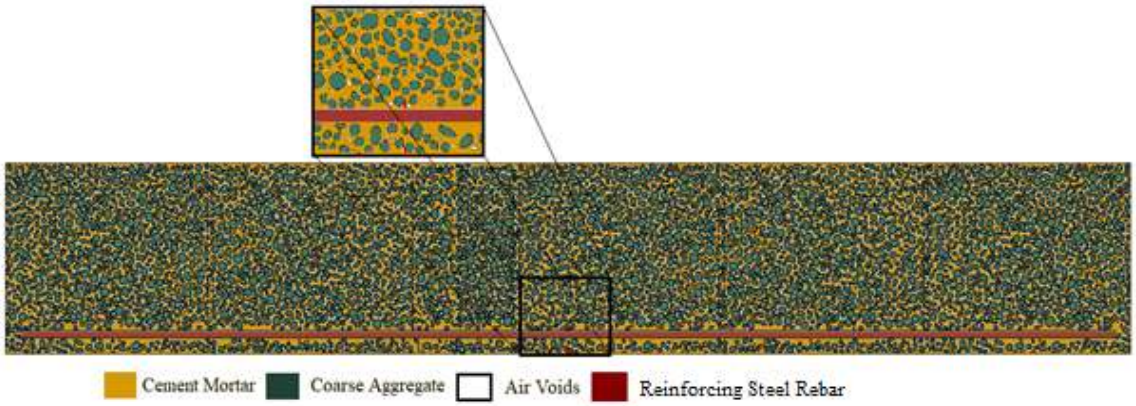

Figure 6. Mesoscale finite element modeling for rounded coarse aggregate with maximum size 20.

To model the coarse aggregate realistically, the aggregate should be distributed randomly according to the grading. The coarse aggregate used in the model is of the same amount used in the mix design.
To calculate the amount of the coarse aggregate in 2D, the area of aggregate in the longitudinal section (L × W) (2200 × 350 mm) for each gradient should be calculated following the steps given below.

Where:
L: Length of the beam, W: Width of the beam
The volume of the sample $V = L \times W \times T = 2.2 \times 0.35 \times 0.2 = 0.154\ m^3$ (6)
Where:
T: third dimension (thickness of the beam)
Area of the sample $A = L \times W = 2.2 \times 0.35 = 0.77\ m^2$ (7)
Calculate the amount of aggregate used in the mixture CA_{wt}
$CA_{wt} = V \times Ag_c \quad (Kg)$ (8)

Where: Ag_c is the coarse aggregate weight in kg/m^3 used in the mix design, equals to 1249 kg/$m^3$when using coarse aggregate with a maximum size of 25 mm, and is equal to 1180 kg/m^3 for coarse aggregate with a maximum size of 20 mm
The absolute volume of aggregate used in the model is calculated as:

$$CA_{Vol} = \frac{CA_{wt}}{density\,of\,\text{aggregate}} = \frac{CA_{wt}}{G_s \times 10^3} \quad (m^3) \tag{9}$$

Where $G_s$represents the specific gravity of the coarse aggregate
Calculate the area of aggregate used in the model in 2D

$$CA_{area} = \frac{CA_{Vol}}{The\,third\,dimension\,of\,the\,model} \quad (m^2) \tag{10}$$

This area is the total area calculated. However, it is needed to find the area for each gradient.
The area of aggregate for each gradient of maximum size 25mm and 20mm in the 2D model is shown in **Tables 2** and **3**, respectively.

Table 2. Area of rounded coarse aggregate for each gradient to a maximum size of 25 mm.

Sieve size, mm	Standard Passing, % according to ASTM C33	Passing %	Retained %	Area for each gradient mm^2 (Retained $\% \times CA_{area}$)
25	100.00	0	0	0
19.00	90 to 100	91.21	8.79	32523
9.50	20 to 55	24.45	67.76	250712
4.75	0 to 15	1.75	22.7	83990
2.36	≈0	0.39	1.36	5032
1.18	≈0	0.37	0.02	74

Table 3. Area of rounded coarse aggregate for each gradient to a maximum size of 20 mm

Sieve size, mm	Standard Passing, % according to ASTM C33	Passing %	Retained %	Area for each gradient mm^2 (Retained $\% \times CA_{area}$)
19.00	100	100	0	0
9.50	40 to 70	45.72	54.28	189980
4.75	0 to 15	0.76	44.96	157360
2.36	0 to 5	0	0.76	2660
1.18	≈0	0	0	0

Air voids content was assumed to equal to the theoretically assessed percentages given in (ACI 211-02, 2002) for the design mix properties. Air voids content percentage equals 1.5% and 2% for the beams have a maximum size of coarse aggregate particles of 25 and 20 mm, respectively. EXCEL sheets were used to calculate the area required for drawing the rounded aggregates. To model the rounded aggregate and air voids, they were assumed of elliptical shapes, as this representation is more accurate because the rounded aggregate is not necessarily a circle.
The ABAQUS software program was used in the modeling and analysis of the RC specimens. Cement mortar and aggregate materials were represented as a linear elastic material. Materials' properties fed to the ABAQUS program are explained in **Table 4.(Wang et al., 2015)**.

Table 4. Materials'properties input in the ABAQUS program

Material	Modulus of Elasticity MPa	Poisson's Ratio	Fracture Energy N-mm/mm2
Aggregate	75000	0.2	-
Mortar	25000	0.2	0.06
Steel	200000	0.3	-

6. RESULTS AND DISCUSSION

A 2D plane stress approach was used to analyze the flexural members (reinforced concrete beams) tested under two-point loading. The non-homogeneity of concrete is taken into account using the mesoscale–model. Then, the numerical results are compared with the experimental results.
Table 5. shows the experimental and numerical maximum applied load for RC beams. The serviceable load is expected to be between 60 and 70% for the ultimate load. In this study, 70% of the ultimate was taken as a serviceable load to measure the percentage of convergence between the experimental and numerical works.

Table 5. The maximum applied load

Beam No.	Maximum Size of Coarse Aggregate	Ultimate Load (kN) In The Experimental Work	Maximum Applied Load (kN) In The Numerical Analysis
1	25	106	120
2	20	99.8	119.87

Fig. 7 and **8** show the load-deflection curve at the mid-span, and the tensile strain curve measured at the mid-span using strain gage, respectively, for rounded coarse aggregate with different maximum sizes.

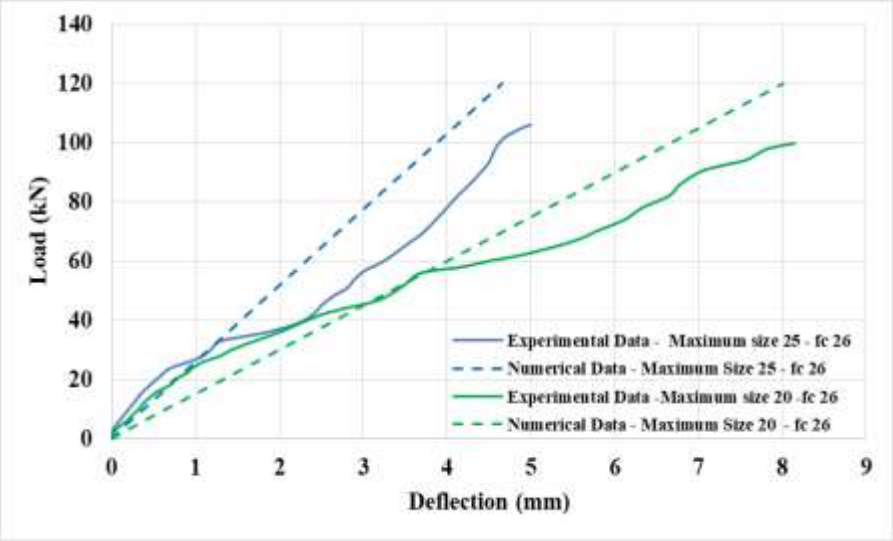

Figure 7. Load-deflection curve at the mid-span of the beams.

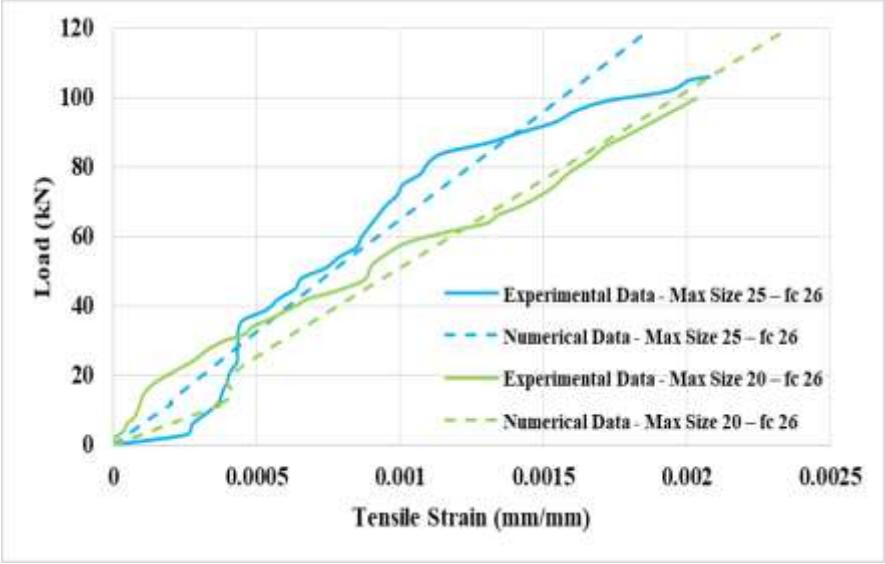

Figure 8. The tensile strain curve at the mid-span.

Fig. 7 shows the maximum deflection in the experimental work at the ultimate load is equal to 5 mm and 8.2 mm for first and second beam, respectively. Also, it can be seen that the experimental deflection approximately has the same amount of deflection until 40 kN, while

when increasing load from this amount, the deflection of the second beam is increased if compared with the other one. From the above, it can be noted that the amount of deflection increases with the decrease of the coarse aggregate maximum size when compared with the deflection at the same load.
When comparing the experimental with the numerical mesoscale modeling that has the same maximum sizes at the serviceable load, the percentage of convergence equal to 74% and 80% for maximum sizes of 25 mm and 20 mm, respectively.
Fracture mechanics is the material mechanical behavior when subjected to load in the presence of cracks **(Hamed et al., 2016)**. The fracture energy of the material can be calculated by computing the area under the stress-deflection curve **(Bažant1992)**.

The first beam (beam No.1) has the upper values of the fracture energy because it has the most significant values, of coarse aggregate (1249 kg/m^3), **Table 1.** This is due to the fracture energy increases with the increase in coarse aggregate content. Because the cracks need to travel around the coarse aggregate particles, in this case, area of the crack surface increases, that led to increasing the energy required for crack propagation that means the fracture toughness increase with an increase in aggregate size **(Moavenzadeh and Kuguel, 1969)**. In addition to the fracture, energy decreases when increasing in porosity that makes the cross-sectional area to be fractured smaller. Porosity in the first beam (beam No.1) where the air void contains is equal to 1.5%, **Table 1, (Ioan et al., 2015),** and the fracture toughness increases with a decrease in the water-to-cement ratio **(Nallathambi et al., 1984)**.

From **Fig. 8**, it can be seen that the experimental results are closer to the numerical results, where the percentage of convergence between them is equal to 92% and 98% for maximum sizes of 25 mm and 20 mm, respectively. Also, it can be noted that the amount of tensile strain in the RC beam at the mid-span increases with the decrease of the coarse aggregate maximum size in both experimental and numerical analysis.

Fig. 9 explains the sections taken to measure the bending and shear stresses developed in the RC beams. **Fig. 10** and **Fig. 11** show the distribution of bending stress across the section A-A taken at the middle part of the beam for rounded coarse aggregate with a maximum size of 25 mm and 20 mm, respectively. While **Figs. 12** and **13** show the shear stresses in MPa at section B-B for RC beams that have a maximum size of 25 mm and 20 mm, respectively.

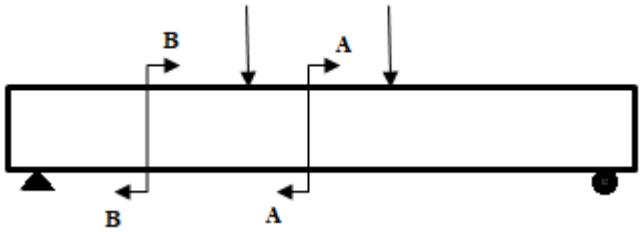

Figure 9. Sections used to calculate the bending and shear stresses.

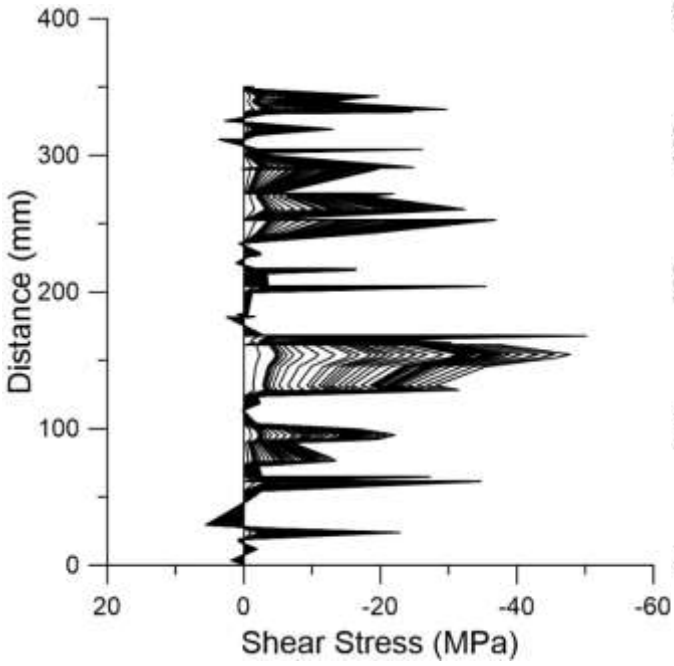

Figure 10. Shear stress for maximum size 25 of mm .

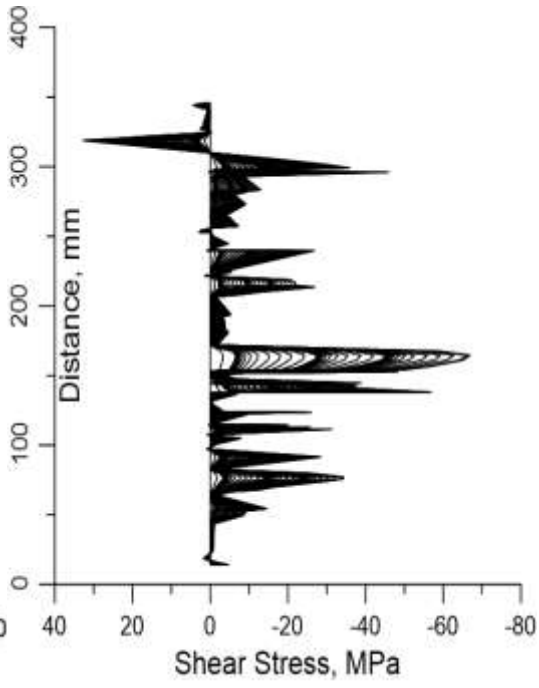

Figure 11. Shear stress for maximum size of 20 mm.

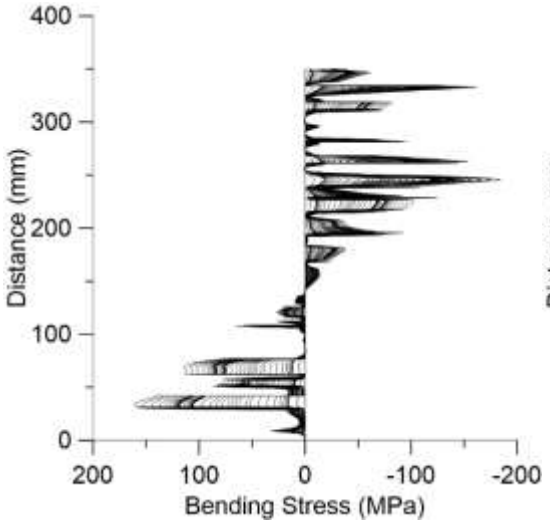

Figure 12. Bending stress for maximum size of 25 mm.

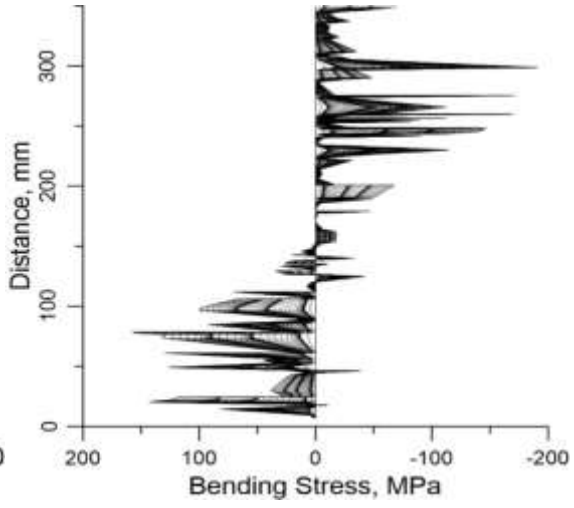

Figure 13. Bending stress for maximum size of 20 mm.

The zigzag shape of the bending and shear stresses may be imputed to the effect of the non-homogeneity of the concrete material. The coarse aggregate particles and air voids near and at the section of the beam causes stress concentration problems at the place of interface position, as can be seen in the above-mentioned figures. The high values of stress due to stress concentration problems, that result from two reasons. The first reason the Modulus of Elasticity for aggregates is three times larger than mortar. The second reason is assumed fully bound (tied) between the

aggregate and cement mortar (at the interface points) in this place; the internal stress values will increase.

7. CONCLUSIONS

- The effect of the non-homogeneity and discontinuity in the concrete material studied using a mesoscale FE model, which was found a powerful method for concrete modeling.
- The random size and distribution of the coarse aggregate particles and air voids have effects on the bending and shear stress distribution in the cross-sections of the models. These effects also include the maximum bending and shear stress and the post-peak of the bending and shear stress with more sensitively to that effects.
- The numerical analysis for the tensile strain behavior of the mesoscale model gave about more than 90% convergence with the experimental data.
- The XFEM was found as a powerful method for the treatment of discontinuity problems that appeared during the fracture process in concrete and bi-material problems.

8. REFERENCES

- ACI 211-02. (2002). "Standard practice for selecting properties for normal, heavyweight, and mass concrete. American Concrete Institute.
- Ahmed. A. 2009. Extended Finite Element Method (XFEM)- Modeling arbitrary discontinuities and Failure analysis. Istituto Universitario Di StudiSuperiori Di Pavia. Book.
- Al-Zuhairi, A. H., and Taj A. I.(a). 2018. Finite element analysis of concrete beam under flexural stresses using mesoscale model. *Civil Engineering Journal*,*4(6)*, pp.1288-1302.
- Al-Zuhairi, A., and Taj, A(b). 2018. Effectiveness of Mesoscale Approach in Modeling of Plain Concrete Beam. *Journal of Engineering*. 24(8), pp.71-80.
- ASTM C33 / C33M-16, (2016). "Standard Specification for Concrete Aggregates, ASTM International", West Conshohocken, PA, www.astm.org, doi: 10.1520/C0033_C0033M-16.
- Bažant, Z. P., (1992). Fracture Mechanics of Concrete Structures. Proceedings of the First International Conference on Fracture Mechanics of Concrete Structures (FraMCoS1), held at Beaver Run Resort, Breckenridge, Colorado, USA, 1-5 June 1992 (Vol. 1). CRC Press.
- Belytschko, T., and Black, A.T., 1999. Elastic Crack Growth in Finite Elements With Minimal, *International Journal For Numerical Methods in Engineering, 45(5)*.pp. 601-620.
- Bentz, D.P., Garboczi, E.J., Jennings, H.M. and Quenard, D.A., 1994. Multi-scale digital-image-based modeling of cement-based materials. *MRS Online Proceedings Library Archive*,370.
- Hamed M. H. AL-Hamdou., Abdel –HaqhadiAbdel-Ali, and Mohammed Z. Mohamedmeki. 2016. Fracture properties of local asphalt concrete. *Journal of Engineering*. 22(7), pp.118-141.
- Ioan D. Marinescu, Mariana Pruteanu (2015) "Deformation and Fracture of Ceramic Materials", Handbook of Ceramics Grinding and Polishing,
- Jivkov, A.P., Engelberg, D.L., Stein, R., &Petkovski, M., 2013. Pore space and brittle damage evolution in concrete. *Engineering Fracture Mechanics, 110 ed*, pp 378-395.

- Khoei, A.R, 2015. *Extended Finite Element Method Theory and Application*. John Wiley and Sons, Ltd.
- Liao, K.Y., Chang, P.K., Peng, Y.N. & Yang, C.C., 2004. A study on characteristics of interfacial transition zone in concrete. *Cement and Concrete Research*, 34(6), pp. 977-989.
- Moavenzadeh, F. and Kuguel, R. (1969) "Fracture of Concrete," Journal of Materials, JMLSA, V. 4, No.3, pp. 497-519.
- Mostafavi, M., Baimpas, N., Tarleton, E., Atwood, R.C., McDonald, S.A., Korsunsky, A.M., and Marrow, T.J., 2013. Three-dimensional crack observation, quantification, and simulation in a quasi-brittle material. *Acta Materialia, 61(16),* pp. 6276-6289.
- Murayama, Y., 2001. *Mesoscopic Systems Fundamentals and Applications*. Verlag Berlin GmbH, Germany: WILEY-VCH.
- Nallathambi, P., Karihaloo, B. L., and Heaton, B. S. (1984) "Effect of Specimen and Crack Sizes, Water/Cement Ratio and Coarse Aggregate Texture upon Fracture Toughness of Concrete," Magazine of Concrete Research, V. 36, No. 129, pp. 227-236.
- Nitka, M. and Tejchman, J., 2015. Modeling of concrete behaviour in uniaxial compression and tension with DEM, *Granular Matter, 17(1),* pp.145-164.
- Schlangen, E., and E.J. Garboczi. 1997. Fracture Simulations of Concrete Using Lattice Models: Computational Aspects. *Engineering Fracture Mechanics57(2-3)*, pp. 319–332
- Wang, X., Yang, Z., Yates, J., Jivkov, A., and Zhang, C., 2015. Monte Carlo Simulations of mesoscale fracture modeling of concrete with random aggregate and pores. *Construction and Building Materials, 75,* pp. 35-45.
- Wang, Xiaofeng, Mingzhong Zhang, and Andrey P. Jivkov. 2015. Computational Technology for Analysis of 3D Meso-Structure Effects on Damage and Failure of Concrete. *International Journal of Solids and Structures, 80,*pp. 310–333.
- Yang, Z.J., X.T. Su, J.F. Chen, and G.H. Liu. 2009. Monte Carlo Simulation of Complex Cohesive Fracture in Random Heterogeneous Quasi-Brittle Materials. *International Journal of Solids and Structures46(17),* pp. 3222–3234.